Author's Copy

Biol. Chem., Vol. 391, pp. 549–559, May 2010 • Copyright © by Walter de Gruyter • Berlin • New York. DOI 10.1515/BC.2010.051

Detection and in-cell selectivity profiling of the full-length West Nile virus NS2B/NS3 serine protease using membrane-anchored fluorescent substrates

Stephanie A. Condotta, Morgan M. Martin[a], Martine Boutin and François Jean*

Department of Microbiology and Immunology, Life Sciences Center, the University of British Columbia, 2350 Health Sciences Mall, Vancouver V6T 1Z3, Canada

* Corresponding author
e-mail: fjean@interchange.ubc.ca

Abstract

Flaviviral NS2B/NS3 heterocomplex serine proteases are a primary target for anti-flavivirus drug discovery. To gain insights into the enzymatic properties and molecular determinants of flaviviral NS2B/NS3 protease substrate specificity in host cells, we developed and applied a novel series of membrane-anchored red-shifted fluorescent protein substrates to detect West Nile virus (WNV) NS2B/NS3 endoproteolytic activity in human cells. The substrate consists of a fluorescent reporter group (DsRed) tethered to the endoplasmic reticulum membrane by a membrane-anchoring domain. Between the two domains is a specific peptide linker that corresponds to the NS2A/NS2B, NS2B/NS3, NS3/NS4A, and NS4B/NS5 protein junctions within the WNV polyprotein precursor. When the protease cleaves the peptide linker, the DsRed reporter group is released, changing its localization in the cell from membrane-bound punctate perinuclear to diffuse cytoplasmic. This change in protein location can be monitored by fluorescent microscopy, and cleavage products can be quantified by Western blotting. Our data demonstrate the robustness of our *trans*-cleavage fluorescence assay to capture single-cell imaging of membrane-associated WNV NS2B/NS3 endoproteolytic activity and to perform in-cell selectivity profiling of the NS2B/NS3 protease. Our study is the first to provide cellular insights into the biological and enzymatic properties of a prime target for inhibitors of WNV replication.

Keywords: cell-based fluorescence assay; flavivirus NS3 protease; NS2B/NS3 protease; viral protease; West Nile virus; West Nile virus NS3 protease.

[a] Present address: Department of Neurology, Center for Neurologic Diseases, Brigham and Women's Hospital and Harvard Medical School, 77 Avenue Louis Pasteur, Boston, MA 02115, USA.

Introduction

West Nile virus (WNV) (family *Flaviviridae*, genus *Flavivirus*) can cause a potentially fatal infection and has posed a serious health concern in North America since its introduction in 1999 (Centers for Disease Control and Prevention, 1999). WNV is a zoonotic pathogen that is maintained in an enzootic cycle involving a mosquito vector and an amplifying bird host. Mammals such as humans and horses are incidental dead-end hosts, as viral titers do not reach levels that permit transmission back to mosquitoes (Drebot et al., 2003). Although WNV is a serious public health problem, no antiviral therapies or vaccines are currently available. Understanding the virus life cycle is essential for the design of an effective therapy.

WNV is a small (approximately 50 nm) enveloped virus with a single-stranded plus sense RNA genome (Castle et al., 1985, 1986; Yamshchikov and Compans, 1993; Lindenbach et al., 2007). Upon uncoating, the viral genomic RNA is translated into a single polyprotein precursor composed of ten viral proteins (Brinton, 2002). The structural proteins [capsid (C), pre-membrane (prM), and envelope (E)] are located at the N-terminal and the nonstructural (NS) proteins are located at the C-terminal in the following order: 5′-UTR-C-prM-E-NS1-NS2A-NS2B-NS3-NS4A-NS4B-NS5-UTR-3′ (Castle et al., 1985, 1986; Rice et al., 1985; Castle and Wengler, 1987; Brinton, 2002). Within the *Flavivirus* genus, *in vitro* studies suggest that host proteases and the viral protease heterocomplex, NS2B/NS3 protease, cleave within the polyprotein precursor at specific sites (Chambers et al., 1990b; Wengler et al., 1991; Cahour et al., 1992; Amberg et al., 1994). The NS2B/NS3 protease recognizes and cleaves C-terminally to highly conserved dibasic residues followed by a small side-chain residue, at protein junctions NS2A/NS2B, NS2B/NS3, NS3/NS4A, and NS4B/NS5 (Chambers et al., 1990b; Wengler et al., 1991; Yamshchikov and Compans, 1993). The remaining viral proteins are released following cleavage by host proteases (Cahour et al., 1992; Falgout and Markoff, 1995; Yu et al., 2008). These proteolytic processing events are essential for the virus life cycle (Chambers et al., 1990b), making the NS2B/NS3 protease an appealing antiviral target.

The NS2B/NS3 protease is composed of two viral proteins: NS2B and NS3. The complex molecular interplay between the viral cofactor NS2B and the NS3 bifunctional enzyme [protease (NS3pro) and helicase (NS3hel): NS3pro-hel] have been a major challenge in studying these induced-fit viral proteases (Richer et al., 2004; Hamill and Jean,

Author's Copy
Author's Copy
Author's Copy

Author's Copy

2005; Martin and Jean, 2006). In the N-terminus of NS3 is a 180-amino acid serine protease domain (NS3pro), which contains the classic catalytic triad of serine proteases, histidine-aspartic acid-serine, at residues 51, 75, and 135, respectively (Bazan and Fletterick, 1989; Gorbalenya et al., 1989a; Wengler et al., 1991); and C-terminal is a helicase/ATPase domain (NS3hel) (Gorbalenya et al., 1989b; Wengler, 1991).

Many studies have shown that the viral protein NS2B is required for NS3 protease activity (Chambers et al., 1991, 1993; Clum et al., 1997; Brinkworth et al., 1999; Yusof et al., 2000). Hydrophobicity profiles of NS2B illustrate a central hydrophilic region flanked by hydrophobic regions, which are thought to associate NS2B to the endoplasmic reticulum (ER) membrane (Wengler et al., 1990; Clum et al., 1997; Yamshchikov et al., 1997; Brinkworth et al., 1999; Lindenbach et al., 2007). Deletion studies have demonstrated that 40 amino acids from the central hydrophilic region of NS2B are sufficient for the proteolytic activity of the protease domain of NS3 (Chambers et al., 1991, 1993; Clum et al., 1997; Brinkworth et al., 1999; Yusof et al., 2000).

In vitro studies have exploited this and have investigated protease activity using truncated bacterial-expressed recombinant forms of the NS2B and NS3 proteins (Nall et al., 2004; Chappell et al., 2005; Shiryaev et al., 2007a). The 40-amino acid hydrophilic domain of NS2B ($NS2B_{40}$) is linked with a glycine-serine linker to the protease domain of NS3 (NS3pro), generating a recombinant $NS2B_{40}$-G_4SG_4-NS3pro protein (Nall et al., 2004; Chappell et al., 2005; Shiryaev et al., 2007a). As a consequence, the flanking N- and C-terminal hydrophobic domains of NS2B and the helicase/ATPase domain of NS3 are omitted, therefore artificially producing the viral protease complex. In addition, these assays use synthetic chromogenic and fluorescent peptidyl-substrates with four or six amino acid peptides containing a chromogenic or fluorogenic group at the P1′ position (Schechter and Berger, 1967), which presents serious limitations for probing the contributions of residues at the C-terminus of the scissile peptide bond to the enzyme specificity (Hamill and Jean, 2005). Furthermore, optimal conditions for detecting protease activity *in vitro* occur at alkaline pH and with the addition of glycerol and detergents (Nall et al., 2004; Chappell et al., 2005; Shiryaev et al., 2007a).

Although *in vitro* assays have been very informative and have helped elucidate some of the important residues of NS2B and NS3 involved in NS2B/NS3 intrinsic enzymatic properties, these studies remain limited. Assays using recombinant truncated forms of NS2B and NS3 do not take into account the potential contributions of other nonstructural protein domains (e.g., NS3hel, NS2B N-terminal domain, and NS2B C-terminal domain) to the enzymatic properties of NS3pro. Furthermore, the complexity of the intracellular environment including the effects of membrane anchoring on protease activity is not considered.

To this effect, it has been shown *in vitro* that the addition of microsomal membranes enhances the efficiency of cleavage by the WNV NS2B/NS3 protease (Wengler et al., 1991; Yamshchikov and Compans, 1994) and by the related Dengue virus, suggesting that membrane association affects protease activity (Clum et al., 1997). Importantly, flaviviral NS2B/NS3pro-hel molecules are localized with the virus-induced membrane-bound replication complexes in the host cytoplasm (Uchil and Satchidanandam, 2003; Lindenbach et al., 2007; Chernov et al., 2008), making the studies of these serine proteases *in cellulo* extremely challenging.

To address these issues, we developed a cell-based *trans*-cleavage assay for the detection of full-length WNV NS2B/NS3pro-hel endoproteolytic activity using ER membrane-anchored red-shifted fluorescent substrates. The substrates consist of an ER membrane-anchoring domain, a protease-specific cleavage sequence, and a DsRed fluorescent reporter group. When the protease cleaves the specific sequence, the DsRed reporter group is released, changing its localization in the cell from membrane-bound punctate perinuclear to diffuse cytoplasmic. This change in protein location can be monitored by fluorescent microscopy, and cleavage products can be detected and quantified with Western blot analysis. We examined the WNV NS2B/NS3 cleavage activities against our internally consistent set of ER membrane-anchored red-shifted fluorescent substrates encoding for the proprotein cleavage sequences that correspond to the protein junctions NS2A/NS2B, NS2B/NS3, NS3/NS4A, and NS4B/NS5 within the WNV polyprotein precursor. In-cell selectivity profiling of the NS2B/NS3 serine protease demonstrated that only the NS4B/NS5 protein junction sequence is significantly cleaved compared with controls under our experimental conditions. Interestingly, as opposed to what has been reported *in vitro* (Nall et al., 2004), all other WNV proprotein junction sequences tested *in cellulo* were not significantly cleaved in *trans* by NS2B/NS3pro-hel compared with controls.

Our data demonstrate the robustness of our *trans*-cleavage fluorescence-based assay to capture single-cell imaging of membrane-associated WNV NS2B/NS3 endoproteolytic activity. Importantly, our work reveals that within the intracellular environment of host cells, the WNV NS2B/NS3 heterocomplex serine protease presents an unexpected substrate selectivity underlying the importance of developing membrane-targeted activity-based probes to study these complex induced-fit viral proteases associated with the ER-anchored replication complexes during flavivirus infection.

Results

Development of novel membrane-anchored red-shifted fluorescent protein substrates to detect WNV NS2B/NS3 endoproteolytic activity in human cells

One of the major goals of this study was to generate a cell-based *trans*-cleavage assay for monitoring the endoproteolytic activity of the WNV NS2B/NS3pro-hel. We cloned the full-length WNV NS2B/NS3 polyprotein into the pFLAG-myc-CMV™-20 epitope mammalian expression vector (Figure 1A). The NS3 protein contains the classic catalytic triad of serine proteases, histidine-aspartic acid-serine, located within the protease domain at residues 51, 75, and 135,

Author's Copy
Author's Copy
Author's Copy

Author's Copy

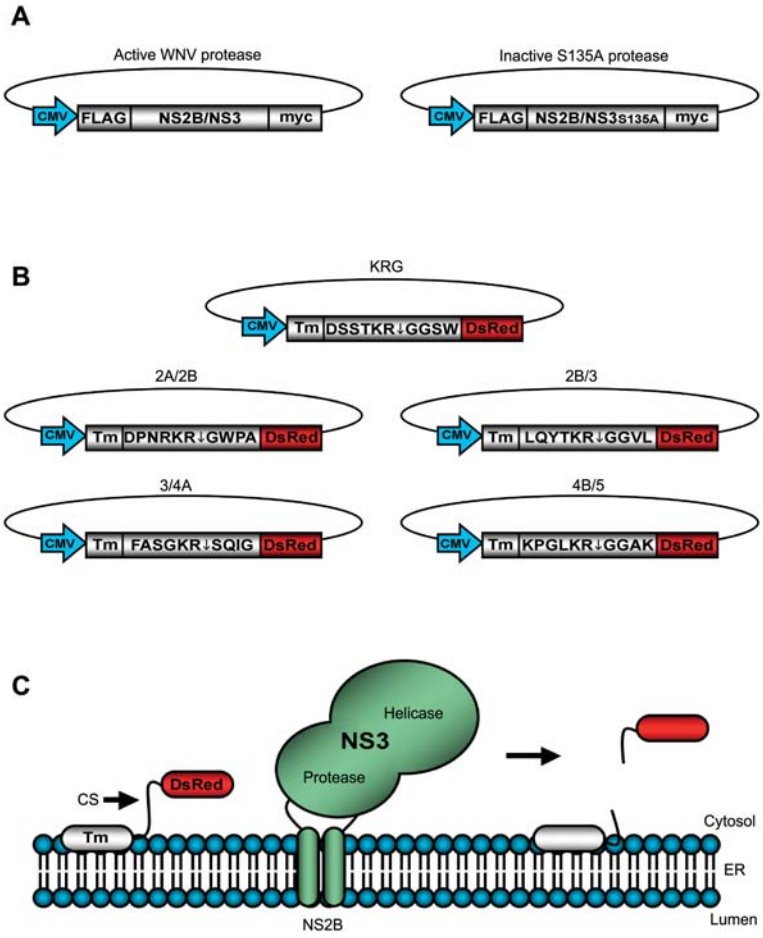

Figure 1 Cell-based *trans*-cleavage assay for detection of the full-length WNV NS2B/NS3pro-hel endoproteolytic activity.
(A) Schematic of WNV protease plasmids. The full-length NS2B/NS3 was cloned into the pFLAG-myc-CMV^{TM}-20 expression vector. Serine 135 within the catalytic triad of NS3 was mutated to alanine. Wild type NS2B/NS3 protease is referred to as active WNV protease and the S135A mutant is referred to as inactive S135A protease. (B) Schematic of substrate plasmids. Each substrate plasmid contains the ER membrane-anchoring domain (Tm), a specific cleavage sequence (CS) that includes the P6-P1↓P1′-P4′ residues and a fluorescent reporter group (DsRed). The KRG substrate was generated from the pTm-DSSTPS↓SGSW-DsRed plasmid described previously (Martin and Jean, 2006). The WNV junction site substrate plasmids were generated from the KRG substrate plasmid and correspond to the protein junction sites NS2A/NS2B (2A/2B), NS2B/NS3 (2B/3), NS3/4A (3/4A), and NS4B/NS5 (4B/5). (C) Schematic representation of the membrane-anchored cell-based fluorescent substrate assay. Protein topology is depicted respective to the ER membrane. The WNV NS2B/NS3 protease associates with the ER membrane through the hydrophobic domains of NS2B. Intact substrate produces a perinuclear punctate DsRed protein pattern at the ER membrane. Upon cleavage sequence processing, DsRed is released from the ER membrane, resulting in a diffuse cytoplasmic DsRed protein pattern. Change in protein location can be monitored with fluorescence microscopy. Adapted from Martin and Jean (2006) and Lindenbach et al. (2007).

respectively (Bazan and Fletterick, 1989; Chambers et al., 1990a; Wengler et al., 1991). We used site-directed mutagenesis to mutate residue serine 135 to alanine (S135A) (Figure 1A). No autocatalytic cleavage products were detected in the S135A mutant compared to wild type, indicating that this mutation rendered the NS2B/NS3 protease catalytically inactive (data not shown), which is consistent with previous reports (Chappell et al., 2005; Bera et al., 2007).

The membrane-bound fluorescent substrates consist of a fluorescent reporter group, DsRed, tethered to the ER membrane by a membrane-anchoring domain (Tm) [Tm is the hepatitis C virus (HCV) NS5A N-terminal amphipathic α-helix amino acid residues 1–34; see Martin and Jean, 2006]. Between Tm and DsRed is a cleavage sequence comprising 10 amino acids corresponding to P6-P1↓P1′-P4′ residues (Figure 1B). For cleavage to occur, there is a critical requirement for colocalization of both the substrate and protease within the cell (Martin and Jean, 2006). That is, the substrate cannot be cleaved unless the protease encounters the substrate at the ER membrane allowing the initial protease-substrate complex and subsequent endoproteolytic cleavage of the substrate, resulting in the release of the enzymatic reaction product from the ER membrane. Intact fluorescent substrate is localized perinuclear, observed as a punctate pattern of DsRed at the ER membrane, whereas the cleaved fluorescent reaction product displays a diffuse cytoplasmic DsRed pattern (Figure 1C) that can be monitored with fluorescent microscopy in intact cells.

Author's Copy
Author's Copy
Author's Copy

Author's Copy

The parent substrate plasmid (pTm-DSSTPS↓SGSW-DsRed) was generated previously for the NS3/NS4A heterocomplex serine protease of HCV (Martin and Jean, 2006). The NS3 protease of HCV has a preferred cleavage sequence of (D/E)XXXX(C/T)↓(S/A) (Grakoui et al., 1993; Richer et al., 2004), whereas the NS3 protease of WNV has a cleavage sequence preference of (K/R)R↓GG (Shiryaev et al., 2007b). We modified the P2P1↓P1′ residues with three sequential rounds of site-directed mutagenesis to generate the substrate pTm-DSST**KR↓G**GSW-DsRed (Figure 1B; KRG).

With the recent demonstration by Hinson and Cresswell that the N-terminal amphipathic α-helices of viperin and HCV NS5A (Tm) that are responsible for the ER localization of both cellular and viral protein in host cells are also necessary and sufficient to localize both proteins to lipid droplets, we investigated the subcellular localization of the KRG membrane-anchored fluorescent substrate within intact cells using markers for ER membrane (anti-calnexin antibody) and lipid droplets (anti-ADRP antibody; Figure 2) (Hinson and Cresswell, 2009).

Using confocal microscopy, we demonstrated a high degree of colocalization between the KRG substrate and the ER endogenous membrane marker calnexin in Huh7 cells (Figure 2; KRG-calnexin-merge) when compared with the relative colocalization of KRG and the lipid droplets endogenous marker ADRP (Figure 2; KRG-ADRP-merge).

We tested for *trans*-cleavage of the KRG substrate by double-transfecting active WNV protease or inactive S135A protease and monitoring cleavage with fluorescent microscopy. A diffuse cytoplasmic DsRed protein pattern was only observed upon transfection of active WNV protease (Figure 3; WNV-DsRed), whereas a perinuclear punctate DsRed pattern was observed with inactive S135A protease (Figure 3; S135A-DsRed) and in substrate-only controls (Figure 3; substrate only-DsRed). Protease expression was confirmed in the active WNV protease and inactive S135A protease samples with immunofluorescent microscopy (Figure 3; myc panel). These results demonstrate that our membrane-anchored cell-based fluorescent substrate assay can be used to monitor the endoproteolytic activity of the WNV NS2B/NS3pro-hel in intact cells. To our knowledge, this is the first experimental evidence demonstrating that the WNV NS2B/NS3 protease is active at the ER membrane using intact cells.

In-cell substrate selectivity of WNV NS2B/NS3 protease

Building from our KRG proof-of-concept study, our next goal was to use our cellular assay to test a series of membrane-anchored fluorescent substrates engineered to present the cleavage sequences of the WNV NS polyprotein precursor that was proposed to be proteolytically cleaved by the NS3 protease. *In vitro* studies suggest that the flaviviral protease cleaves the C-terminal side of dibasic residues at protein junctions NS2A/NS2B, NS2B/NS3, NS3/NS4A, and NS4B/NS5. The P6-P1↓P1′-P4′ amino acid residues found at these protein junctions are DPNRKR↓GWPA, LQYTKR↓GGVL, FASGKR↓SQIG, and KPGLKR↓GGAK, respectively (Figure 1B).

We wanted to evaluate the relative *trans*-cleavage endoproteolytic activity of WNV NS2B/NS3pro-hel when tested using an internally consistent set of membrane-anchored sub-

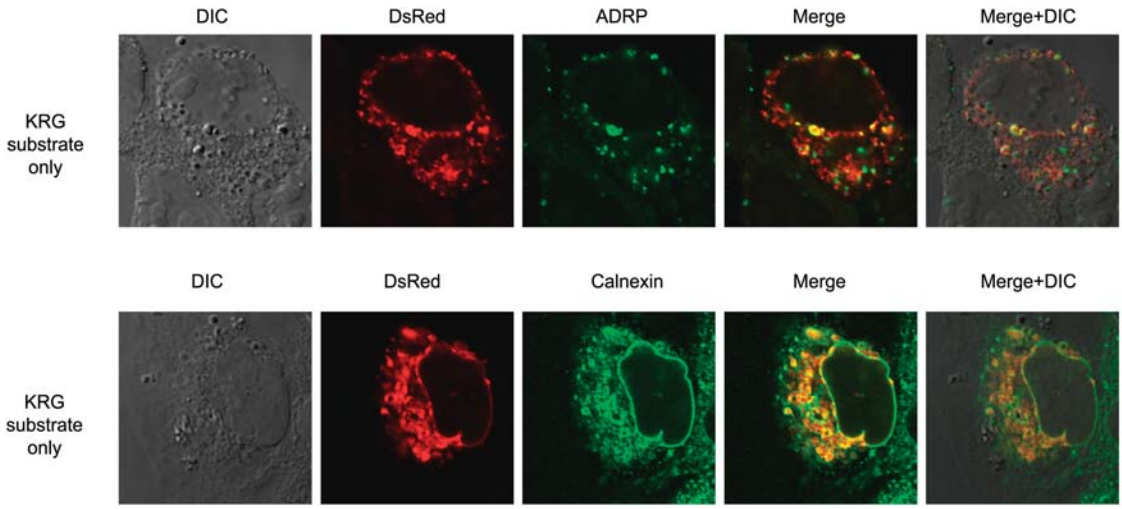

Figure 2 Subcellular localization of KRG substrate.
Huh7 cells were transfected with the KRG substrate and fixed 24 h post-transfection. Cells were probed with either a lipid droplet maker (anti-ADRP monoclonal antibody) or an ER membrane marker (anti-calnexin polyclonal antibody). The KRG substrate DsRed protein pattern was observed using the DsRed signal. Shown is the KRG substrate with lipid droplet marker ADRP (top row) and KRG substrate with ER membrane marker calnexin (bottom row). DIC (differential interference contrast) was acquired at the time of imaging (first column, DIC); the KRG substrate DsRed protein pattern (second column, DsRed) (shown in red); lipid droplet and ER membrane marker (third column, ADRP or calnexin, respectively) (shown in green); merged DsRed and lipid droplet or ER membrane marker (fourth column, merge); merged DsRed, lipid droplet, or ER membrane marker and DIC (last column, merge+DIC). Cells were imaged using a Leica TCS-SP5 confocal microscope (Leica Microsystems).

Author's Copy
Author's Copy
Author's Copy

Author's Copy

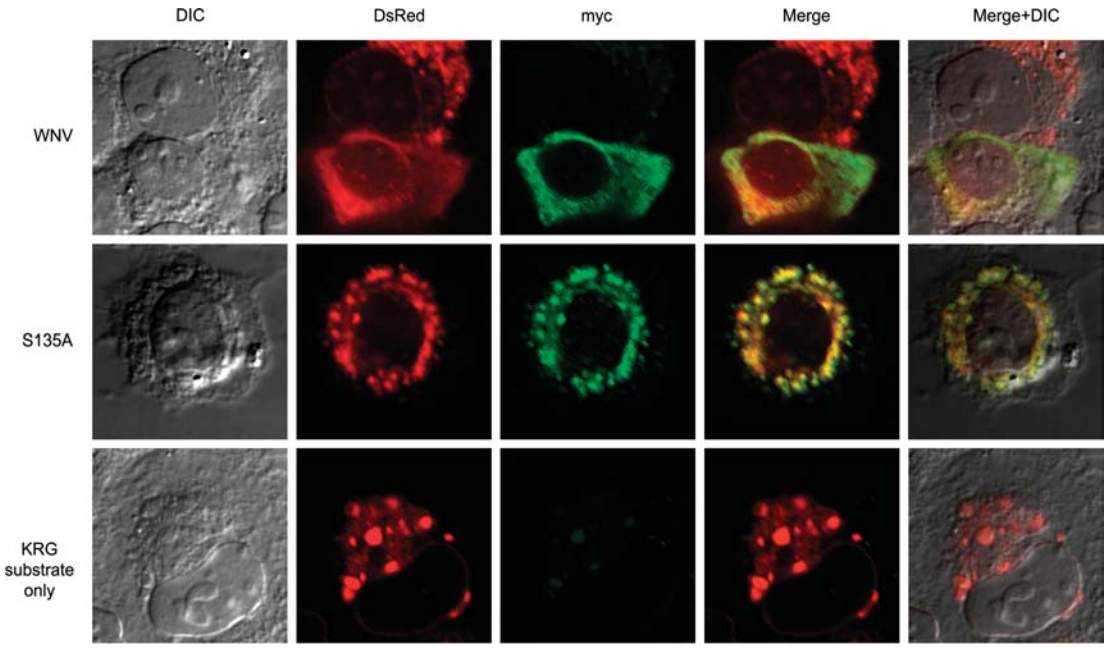

Figure 3 Proof-of-concept: active WNV protease is able to cleave substrate at the ER membrane.
Huh7 cells were double-transfected with active WNV protease and KRG substrate, or with inactive S135A protease and KRG substrate, or single transfection with KRG substrate only. Then 24 h post-transfection, cells were fixed and protease was probed for with anti-myc monoclonal antibody. Processing of the substrate cleavage sequence by the WNV NS2B/NS3 protease was monitored using the DsRed signal. Shown are active WNV protease with KRG substrate (top row), inactive S135A protease with KRG substrate (middle row), and KRG substrate-only control (bottom row). DIC (differential interference contrast) was acquired at time of imaging (first column, DIC). Processing of substrate cleavage sequence (second column, DsRed) (shown in red); protease probe (third column, myc) (shown in green); merged DsRed and myc signal (fourth column, merge); merged DsRed, myc, and DIC (last column, merge+DIC). Cells were imaged with a Leica TCS-SP5 confocal microscope (Leica Microsystems).

Author's Copy

Author's Copy

strates. We modified the cleavage sequence of the KRG substrate with several rounds of site-directed mutagenesis to generate substrates containing the P6-P1↓P1′-P4′ amino acid residues found at these protein junctions (Figure 1B; 2A/2B, 2B/3, 3/4A, 4B/5). We then double-transfected substrates with active WNV protease or inactive S135A protease and monitored cleavage with fluorescent microscopy. A diffuse cytoplasmic DsRed protein pattern was only observed with active WNV protease transfected with the 4B/5 substrate (Figure 4; WNV-4B/5). All other protein junction substrates transfected with active WNV protease, as well as substrates transfected with inactive S135A protease and in substrate-only controls, illustrated a perinuclear punctate DsRed pattern (Figure 4). Protease expression was confirmed with immunofluorescent microscopy in active WNV protease and inactive S135A protease samples (data not shown). The results demonstrate that only the NS4B/NS5 protein junction site can be endoproteolytically cleaved efficiently in *trans* by the WNV NS2B/NS3pro-hel under our experimental conditions.

We next examined substrate cleavage with Western blot analysis and observed that the intact substrate migrated at 34 kDa (Figure 5A; white arrow) and the DsRed-containing cleavage product migrated at 29 kDa (Figure 5A; WNV, black arrow). A faint cleavage band was observed in substrate-only controls and in inactive S135A protease samples (Figure 5; thin black arrow). In the active WNV protease samples, the 4B/5 substrate was processed efficiently compared with the other protein junction site substrates tested with 2A/2B substrate being processed the least. Processing of the KRG substrate was comparable to the 4B/5 substrate (Figure 5A; WNV).

We subsequently quantified and calculated the percent of substrate cleaved from the Western blots by dividing the lower cleavage band signal by the total signal (uncleaved+cleaved) (Figure 5B) (Table 1). In the active WNV protease samples, the 4B/5 substrate had a higher percent of cleavage compared with the other substrates tested (2A/2B=5.0±0.9%; 2B/3=16.0±4.3%; 3/4A=7.5±1.3%; 4B/5=34.5±9.3%) (Figure 5B; WNV, black bars) with significant differences ($p<0.05$) between 4B/5 compared with 2A/2B and 3/4A substrates as well as between controls (S135A=7.0±0.7%; substrate-only=8.2±1.9%) (Figure 5B; S135A, gray bar; substrate-only, white bar). The other protein junction site substrates tested (2A/2B, 2B/3, and 3/4A) were not significant above inactive S135A protease or substrate-only controls (Figure 5B and Table 1). Interestingly, a trend of a lower percent of substrate cleaved was observed in the inactive S135A protease samples (Figure 5B; S135A, gray bars) compared with the substrate-only samples (Figure 5B; substrate-only, white bars), suggesting that the inactive WNV S135A protease forms an initial enzyme-substrate complex that could protect the membrane-anchored substrates from being cleaved by host protease(s) (Table 1).

Author's Copy

Author's Copy

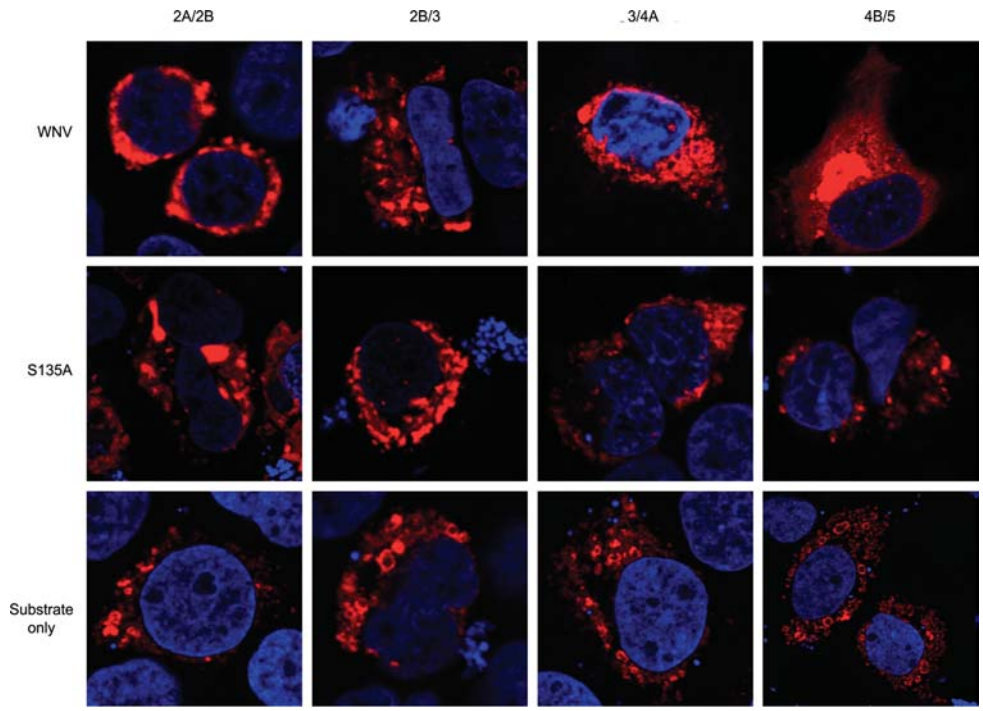

Figure 4 *Trans*-cleavage of fluorescent substrates containing WNV protein junction site sequences.
Huh7 cells were double-transfected with active WNV protease and WNV junction site substrates, or with inactive S135A protease and WNV junction site substrates, or singly with substrate only. Then 24 h post-transfection, cells were fixed and processing of the substrate cleavage sequence was monitored with the DsRed signal (shown in red). Shown are active WNV protease with substrate (top row, WNV), inactive S135A protease with substrate (middle row, S135A), and substrate-only controls (bottom row, substrate-only). Substrates correspond to the WNV protein junction sites NS2A/NS2B (first column, 2A/2B), NS2B/NS3 (second column, 2B/3), NS3/4A (third column, 3/4A), and NS4B/NS5 (fourth column, 4B/5). Nuclei were visualized with Hoechst staining (shown in blue). Cells were imaged with an Olympus Fluoview scanning confocal microscope (Olympus Corporation).

Author's Copy

Author's Copy

In the KRG substrate, significant differences were observed between the active WNV protease compared with the inactive S135A protease and substrate-only samples (WNV=33.5±8.3%; S135A=7.7±1.2%; substrate-only=11.2±0.8%; $p<0.05$). In the active WNV protease samples, no significant differences were observed between the KRG and 4B/5 substrates. The substrates KRG, 4B/5, and 2B/3 all contain the KR↓GG sequence (Figure 1B); however, the 2B/3 substrate was poorly processed compared with the other two (Figure 5B) (Table 1), suggesting that the other residues present in the cleavage sequences tested have an effect on WNV NS2B/NS3 protease substrate selectivity and/or cleavage efficiency.

Discussion

In this study, we report novel membrane-anchored fluorescent substrates for detecting the endoproteolytic activity of the full-length WNV NS2B/NS3pro-hel intracellularly. Our results demonstrate that the substrate that corresponds to the NS4B/NS5 junction site was cleaved in *trans*, whereas the remaining substrates that correspond to the NS2A/NS2B, NS2B/NS3, and NS3/NS4A proprotein junction sites were poorly processed in *trans* under our experimental conditions. To our knowledge, this is the first demonstration that the WNV NS2B/NS3pro-hel is an active endoproteolytic enzyme at the ER membrane and the first study reporting the in-cell selectivity profiling of the membrane-anchored flaviviral protease.

Processing of the polyprotein precursor by the NS2B/NS3 protease is essential in the flavivirus life cycle (Chambers et al., 1990b), and as such, it has been one of the prime antiviral targets for WNV therapy. Typically, *in vitro* substrate assays are used to assess WNV NS2B/NS3 protease activity using the truncated bacterial-expressed recombinant form of the protease, $NS2B_{40}$-G_4SG_4-NS3pro (Nall et al., 2004; Chappell et al., 2005, 2006, 2007, 2008a,b; Shiryaev et al., 2006, 2007a,b,c; Bera et al., 2007; Radichev et al., 2008). Nall et al. (2004) investigated the enzymatic characterization of the WNV recombinant $NS2B_{40}$-G_4SG_4-NS3pro protease *in vitro*. The substrates synthesized were chromogenic hexapeptidyl substrates composed of the P6-P1 residues corresponding to the protein junctions NS2A/NS2B (Ac-DPNRKR-*p*NA), NS2B/NS3 (Ac-LQYTKR-*p*NA), NS3/NS4A (Ac-FASGKR-*p*NA), and NS4B/NS5 (Ac-KPGLKR-*p*NA). The authors ranked the relative substrate processing efficiency based on performance constants (k_{cat}/K_m: M^{-1} s^{-1}) as NS3/NS4A (4222±313)>NS4B/NS5 (1827±124)≥NS2A/NS2B (1756±96)≥NS2B/NS3 (1233±86 units) with NS3/NS4A being

Author's Copy

Author's Copy

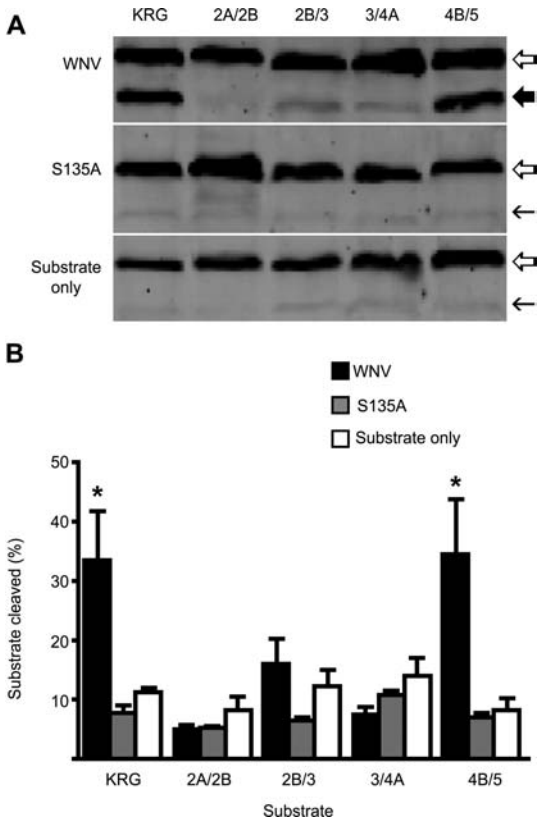

Figure 5 In-cell substrate selectivity profiling of WNV NS2B/NS3 protease.

(A) *Trans*-cleavage of fluorescent substrates detected by Western blot analysis. Huh7 cells were double-transfected with active WNV protease and each substrate, or with inactive S135A protease and each substrate, or singly transfected with substrate only. Then 24 h post-transfection, cells were harvested and whole cell lysates were probed by Western blotting using the anti-DsRed polyclonal antibody. Intact substrate was detected at 34 kDa (white arrow), and cleaved substrate was detected at 29 kDa (black arrow). Shown are active WNV protease with substrate (top row), inactive S135A protease with substrate (middle row), and substrate-only controls (bottom row). Substrates correspond to the KRG substrate (first column, KRG) and the WNV protein junction sites NS2A/NS2B (second column, 2A/2B), NS2B/NS3 (third column, 2B/3), NS3/4A (fourth column, 3/4A), and NS4B/NS5 (last column, 4B/5). (B) Quantification of Western blot analysis. Depicted are percent of substrate cleaved (*y*-axis). Substrates correspond to the KRG substrate and the WNV protein junction site substrates, 2A/2B, 2B/3, 3/4A, and 4B/5 (*x*-axis). Active WNV protease samples (black bars), inactive S135A protease samples (gray bars), and substrate-only samples (white bars). Results shown are the average of four independent experiments run in duplicate. Significance was noted in samples having differences in substrates with active WNV protease compared to substrate with inactive S135A protease and substrate-only controls (*$p<0.05$).

cleaved the best and NS2B/NS3 cleaved the least (Nall et al., 2004).

Shiryaev et al. (2007b) examined the substrate recognition pattern of the WNV recombinant protease $NS2B_{40}$-G_4SG_4-NS3pro *in vitro*. They used fluorescent-biotin tagged octapeptidyl substrates composed of the P4-P1↓P1′-P4′ residues spanning several potential cleavage sites within the WNV polyprotein precursor. They demonstrated that the protease was able to cleave substrates corresponding to the NS2B/NS3, NS4B/NS5, and NS2A/NS2B junction sites; however, no cleavage was detected with the NS3/NS4A peptidyl substrate (relative cleavage efficiencies of 73%, 73%, 64%, 0%, respectively) (Shiryaev et al., 2007b).

On the contrary, our results using decapeptidyl substrates demonstrate that in the context of the host cell, the 4B/5 substrate is the only membrane-anchored red-shifted fluorescent protein substrate efficiently cleaved in *trans* by WNV NS2B/NS3pro-hel under our experimental conditions (Table 1). Interestingly, similar results were demonstrated in a cellular expression system of the related Yellow Fever virus (YFV) (Chambers et al., 1991). Chambers et al. (1991) demonstrated via a vaccinia virus-T7 expression system of YFV that the NS4B/NS5 junction site was efficiently cleaved in *trans*, whereas the NS2A/NS2B and NS3/NS4A junctions were inefficiently cleaved. They suggested that perhaps *cis*-cleavage is preferred at these junction sites (Chambers et al., 1991). Taken together, the results suggest that the membrane microenvironment and/or the other nonstructural protein domains not examined *in vitro* (e.g., NS3hel, NS2B N-terminal domain, and NS2B C-terminal domain) contribute to the flaviviral NS3pro-enzymatic properties in host cells. Alternatively, the experimental conditions used to perform the enzymatic tests *in vitro* such as high pH, the addition of glycerol, and detergents – not used in our cell-based *trans*-cleavage assay – could also explain, in part, the apparent discrepancy between these results obtained using *in vitro* and *in cellulo* enzymatic assays. For example, Ezgimen et al. (2009) recently showed that varying detergents have an effect on the protease activity of WNV. They demonstrated *in vitro* that nonionic detergents such as Triton X-100, Tween, and NP-40 enhanced WNV protease activity 2- to 2.5-fold, ultimately making these detergents unsuitable for drug discovery (Ezgimen et al., 2009).

Another important difference in the experimental design developed in our *in cellulo* study in contrast to *in vitro* studies is the engineering of an internally consistent set of membrane-anchored fluorescent protein substrates encompassing the amino acid residues from P6-P1↓P1′-P4′ around the scissile peptide bond of the WNV nonstructural polyprotein precursor cleavage sites. In general, *in vitro* enzymatic tests are performed using tetrapeptidyl or hexapeptidyl substrates based on the NS2B/NS3 protein junction site (Chappell et al., 2006, 2007; Shiryaev et al., 2006, 2007a,b,c; Chernov et al., 2008). The tetra- and hexa-peptidyl substrates contain a chromogenic or fluorogenic group in the P1′ position; as a consequence, the influence of the residues in the Pn′ position of the cleavage site is not taken into account. Our results obtained using decapeptidyl substrate sequences demonstrated that despite the fact that both the NS2B/NS3 and NS4B/NS5 protein junction sites have the KR↓GG (P2-P1↓P1′-P2′) primary sequence, the 4B/5 substrate was cleaved more efficiently compared with the 2B/3 substrate (Table 1). This strongly suggests that the other residues locat-

Author's Copy
Author's Copy
Author's Copy

Author's Copy

Table 1 Percent of substrate cleaved.

Protease	Substrate				
	KRG	2A/2B	2B/3	3/4A	4B/5
WNV	33.5±8.3*	5.0±0.9	16.0±4.3	7.5±1.3	34.5±9.3*
S135A	7.7±1.2	5.2±0.2	6.5±0.6	10.7±0.7	7.0±0.7
Substrate-only	11.2±0.8	8.2±2.2	12.2±2.6	14.0±2.9	8.2±1.9

Listed are the percent of substrate cleaved as quantified from Western blotting (Figure 5B). Percentages were calculated from the average of four independent duplicate experiments.

*Significance was noted in samples having differences in substrates with active WNV protease compared to substrate with inactive S135A protease and substrate-only controls ($p<0.05$). Statistical analysis was performed with a two-tailed, unpaired Student's *t*-test.

ed within the P6-P1↓P1′-P4′ positions around the scissile peptide bond of the substrates have an effect on *trans*-cleavage and that the WNV NS2B/NS3 protease has broader substrate requirements than previously appreciated. The P6-P1↓P1′-P4′ amino acid residues found at the NS2B/NS3 and NS4B/NS5 junction sites are LQYTKR↓GGVL and KPGLKR↓GGAK, respectively, with differences in amino acid properties occurring at P6, P5, P4, P3, and P4′, suggesting that these residues affect the enzyme-substrate molecular interactions perhaps favoring the NS4B/NS5 protein junction site to be cleaved *in trans*. Interestingly, it has been reported that mutation of certain residues at the YFV proprotein junction sites affect cleavage efficiency and flaviviral polyprotein processing (Lin et al., 1993). Furthermore, Chambers et al. (1995) showed that varying substitutions at the P4-P1′ residues of the NS2B/NS3 junction site of the YFV polyprotein precursor reduced or enhanced cleavage efficiency, suggesting that the wild type residues are not optimal for cleavage by the flaviviral protease (Chambers et al., 1995). In this regard, one might argue that the lack of apparent *trans*-cleavage of the other membrane-anchored fluorescent protein substrates tested in our study could be temporal. Our enzymatic assays were performed at 24 h post-transfection; perhaps this time point could be too early for *trans*-cleavage event to occur efficiently at the other flaviviral proprotein junction sites examined in this study. Taken together, these results underline the importance of the amino acid residues present at the proprotein cleavage sites for the NS2B/NS3 site-specific mediated cleavage events of the viral polyprotein precursor and the resultant intracellular viral protein molarity of the nonstructural flavivirus endoproteolyic products during WNV replication.

Replication of the flaviviral genome takes place within a membrane-associated replication complex that is composed of the viral protein NS5 (the RNA-dependent RNA polymerase) and the helicase/ATPase domain of NS3 (Uchil and Satchidanandam, 2003). The viral proteins NS1, NS2A, and NS4A are thought to be involved in the replication complex although their exact function is still unclear (Uchil and Satchidanandam, 2003). Using the full-length NS2B and NS3 proteins allows us to study the WNV NS2B/NS3 protease with all protein domains considered, allowing for the proper folding and subcellular localization and the effects of membrane anchoring to be taken into account.

NS3, mostly a hydrophilic protein, is predicted to be associated to the ER membrane through its interaction with NS2B, and NS2B is thought to be membrane-associated via its hydrophobic domains (Figure 1C) (Wengler et al., 1991; Lindenbach et al., 2007). Clum et al. (1997) examined the effects of membranes on the viral protease of the related Dengue virus. They demonstrated that the addition of microsomal membranes *in vitro* enhanced the activity of the protease. They concluded that the membrane association of the NS2B protein might influence the activity of the NS3 protease (Clum et al., 1997). In this study, we observed a difference in substrate selectivity compared to *in vitro* conditions, which can be attributed, in part, to the intracellular microenvironment, such as the interplay of membranes on the proper folding and/or function of the WNV NS2B/NS3 heterocomplex serine protease.

In conclusion, we report a novel series of internally consistent sets of ER membrane-anchored red-shifted fluorescent substrates to examine the membrane-associated WNV NS2B/NS3 endoproteolytic activity in host cells. The results of our in-cell selectivity profiling of the full-length WNV NS2B/NS3 serine protease reveal that the viral protease behaves differently within the complex intracellular environment of the host cell compared with *in vitro* conditions, emphasizing the need for cell-based assays for studying flaviviral induced-fit proteases, such as the one described in this report. This assay is an invaluable tool that will significantly advance our understanding of WNV protease biology and allow for the biochemical characterization of the full-length NS2B/NS3pro-hel heterocomplex serine protease in a more physiologically relevant environment. Furthermore, the information obtained will be useful for the rational design of specific flaviviral NS2B/NS3 protease inhibitors that in turn can be validated in our novel cell-based assay.

Materials and methods

Construction of plasmids expressing WNV full-length NS2B/NS3pro-hel

Total RNA was extracted from a WNV bird sample (a kind gift from Dr. Michael A. Drebot, National Microbiology Laboratory,

Author's Copy

Author's Copy

Author's Copy

Public Health Agency of Canada) with an RNeasy Kit (Qiagen, Mississauga, ON, Canada). cDNA was made and the full-length NS2B/NS3pro-hel was cloned into pFLAG-myc-CMV™-20 Expression Vector (Sigma, St. Louis, MO, USA) using the EcoRI and XbaI restriction sites (forward primer: 5′-CGC GAA TTC AGG ATG GCC CGC AAC T-3′; reverse primer: 5′-CCT CTA GAA CGT TTT CCC GAG GC-3′; EcoRI and XbaI restriction sites underlined, respectively). Wild type NS2B/NS3pro-hel was indicated as active WNV protease (Figure 1A). An alanine mutation was generated with site-directed mutagenesis (Stratagene, La Jolla, CA, USA) within the N-terminal serine protease domain of NS3 at the catalytic triad residue serine 135 (S135A) (Bazan and Fletterick, 1989; Wengler et al., 1991; Chappell et al., 2005). Mutation was confirmed by automated sequencing (UBC DNA Sequencing Laboratory, Vancouver, BC, Canada). The S135A mutant was indicated as inactive S135A protease (Figure 1A).

Construction of substrate plasmids expressing WNV nonstructural polyprotein precursor cleavage sites

The parent substrate plasmid contained an ER membrane-anchoring domain (Tm) (N-terminal amphipathic α-helix of HCV NS5A protein amino acid residues 1–34), a protease-specific cleavage sequence that includes the P6-P1↓P1′-P4′ residues (Schechter and Berger, 1967), and a fluorescent reporter group (DsRed-Express, referred to as 'DsRed'), as has been reported previously (Martin and Jean, 2006). pTm-DSSTPS↓SGSW-DsRed was sequentially mutated with site-directed mutagenesis (Stratagene) to generate the substrate plasmid, pTm-DSST**KR**↓**G**GSW-DsRed (designated 'KRG') (Figure 1B). The KRG substrate plasmid was sequentially mutated with site-directed mutagenesis (Stratagene) to generate substrate plasmids containing cleavage sequences corresponding to the protein junctions that are cleaved by the WNV NS2B/NS3 protease within the polyprotein precursor: NS2A/NS2B (pTm-DPNRKR↓GWPA-DsRed), NS2B/NS3 (pTm-LQYTKR↓GGVL-DsRed), NS3/NS4A (pTm-FASGKR↓SQIG-DsRed), and NS4B/NS5 (pTm-KPGLKR↓GGAK-DsRed) (Figure 1B). All mutations were confirmed by automated sequencing (UBC DNA Sequencing Laboratory).

Cell culture

Human hepatocellular carcinoma cells (Huh7 cells) were grown in complete Dulbecco's modified Eagle's medium (DMEM; Gibco/Invitrogen, Burlington, ON, Canada) supplemented with heat-inactivated 10% v/v fetal bovine serum (Gibco/Invitrogen), 50 units/ml penicillin, 50 μg/ml streptomycin, and 100 μM non-essential amino acids (Gibco/Invitrogen). Cells were grown at 37°C in the presence of 5% CO_2.

Fluorescence and immunofluorescence microscopy

Huh7 cells were seeded in 24-well plates on top of a glass coverslip at 20 000 cells/well and grown for 2 d until approximately 60% confluent. Huh7 cells were double-transfected with 1.0 μg of active WNV protease plasmid and 1.0 μg of each substrate plasmid using *Trans*IT-LT1 transfection reagent (Mirus Bio, Madison, WI, USA). Controls included double-transfection of Huh7 cells with 1.0 μg of inactive S135A protease and 1.0 μg of each substrate plasmid or single transfection with 1.0 μg of substrate plasmid. All processing steps were done at room temperature unless otherwise noted. Then 24 h post-transfection, cells were washed two times with 0.5 ml phosphate buffered saline (PBS) and fixed in 3.8% v/v formaldehyde (Fischer Scientific, Pittsburg, PA, USA) in PBS (30 min). Cells were rinsed two times with 0.5 ml PBS. For immunofluorescent microscopy, cells were permeabilized for 30 min in 0.5 ml PBS containing 0.05% w/v saponin (PBS-S) (Sigma-Aldrich Corp., St. Louis, MO, USA). Cells were blocked in 0.2 ml of PBS-S containing 3% w/v bovine serum albumin (BSA) (Sigma-Aldrich) (30 min). For the lipid droplet marker, primary anti-ADRP (adipocyte differentiation-related protein) monoclonal antibody was added directly to cells (ready to use, Progen, Heidelberg, Germany) (60 min). The other primary and all secondary antibodies were diluted in PBS-S containing 3% BSA. For the ER membrane marker, primary anti-calnexin polyclonal antibody was added to cells (1:100, Sigma-Aldrich) for 60 min. For protease detection, cells were probed with primary anti-myc monoclonal antibody (1:100, Stratagene) (60 min). Cells were then washed six times with 0.5 ml PBS-S. Cells were probed with secondary Alexa Fluor-488-conjugated donkey anti-mouse monoclonal antibody or Alexa Fluor-488-conjugated donkey anti-rabbit polyclonal antibody (1:100, Molecular Probes/Invitrogen) (60 min). Cells were washed three times with 0.5 ml PBS-S, then three times with 0.5 ml PBS. Nuclei were stained using 0.5 ml Hoechst stain (Invitrogen; 5 μg/ml, 15 min). Cells were washed three times with 0.5 ml PBS, then two times with 0.5 ml HPLC water (Sigma-Aldrich). Coverslips were removed from 24-well plates and air-dried. Coverslips were mounted with mounting solution containing 2.5% w/v DABCO (1,4-diazabicyclo[2.2.2] octane, Sigma-Aldrich) in 1:10 buffered glycerol and sealed with clear nail polish. Images were acquired using either a Leica TCS-SP5 confocal microscope (Leica Microsystems, Richmond Hill, Canada) or an Olympus Fluoview FV1000 laser scanning confocal microscope (Olympus Canada Inc., Markham, Canada).

Transfections and Western blotting

Six well plates were seeded with Huh7 cells at 200 000 cells/well and grown for 3 d until approximately 80% confluent. Huh7 cells were double-transfected with 2.5 μg of active WNV protease plasmid and 2.5 μg of each substrate plasmid using *Trans*IT-LT1 Transfection Reagent (Mirus Bio). Controls included double-transfection of Huh7 cells with 2.5 μg of inactive S135A protease and 2.5 μg of each substrate plasmid or single transfection with 2.5 μg of substrate plasmid. Then 24 h post-transfection, cells were placed on ice and washed with 3 ml PBS containing 1× protease inhibitor cocktail (PBS-PI) (EDTA-free Complete Protease Inhibitor; Roche, Laval, QC, Canada). Cells were harvested by scraping in 0.5 ml PBS-PI, pelleted (16 110 *g*, 1 min, 4°C), then frozen (-86°C) for Western blot analysis. Cell pellets were resuspended in 0.2 ml hypotonic lysis buffer (20 mM Tris pH 7.4, 10 mM $MgCl_2$, 10 mM $CaCl_2$) containing 1× protease inhibitor cocktail (Roche). Cells were placed on ice and vortexed every 5 min for a total of 15 min. Then, 15 μl of sample was removed, added to 15 μl of 2× SDS-PAGE sample buffer (0.1 M Tris pH 6.8, 20% v/v glycerol, 4% w/v SDS, 0.002% w/v bromophenol blue, 0.7 M 2-mercaptoethanol), and boiled (10 min, 95°C). Then, 20 μl of sample was resolved on a 12% SDS-polyacrylamide gel (110 V, 90 min) and transferred to a nitrocellulose membrane (25 V, 60 min) using a semi-dry electrophoretic transfer system (Bio-Rad Laboratories, Mississauga, ON, Canada). Membranes were rinsed three times in PBS and blocked for 60 min with Odyssey Blocking Buffer (LI-COR Biosciences, Lincoln, NE, USA). The membranes were probed according to Odyssey Infrared Imaging System Western blot analysis protocol (LI-COR Biosciences).

Primary and secondary antibodies were diluted in Odyssey Blocking Buffer (LI-COR Biosciences) containing 0.1% v/v Tween-20 (Sigma-Aldrich). Membranes were probed with primary anti-DsRed polyclonal antibody (1:1000, Clontech Laboratories, Mountain

Author's Copy

Author's Copy

Author's Copy

Author's Copy

View, CA, USA) (60 min). Membranes were washed six times with PBS containing 0.1% v/v Tween-20. Membranes were probed with secondary IRDye 680-conjugated goat anti-rabbit polyclonal antibody (1:10 000, LI-COR Biosciences) (30 min). Membranes were washed six times with PBS containing 0.1% v/v Tween-20, then imaged using an Odyssey Infrared Imaging System (LI-COR Biosciences).

Quantification and statistical analysis

Analysis and quantification of integrated band intensity were performed using the Odyssey Infrared Imaging System application software version 2.1.12 (LI-COR Biosciences). The percent of substrate cleaved was calculated by dividing the cleaved signal by the total signal (cleaved plus uncleaved), thereby normalizing the readout for each sample. Averages were calculated from four independent experiments run in duplicate. GraphPad Prism (GraphPad Software, Inc., La Jolla, CA, USA) was used for graphical representation and statistical analysis. *p*-Values were obtained for two-tailed, unpaired, Student's *t*-test, and significance was considered for $p<0.05$.

Acknowledgments

This work is supported by a Canadian Institutes of Health Research (CIHR) grant MOP-84462 (to F. Jean). M. Martin was supported by a CIHR Doctoral award and a UBC-CIHR translational research in infectious diseases (TRID) scholarship award. We thank Dr. Charles Rice (The Rockefeller University) for the Huh7 cells and Dr. Michael Drebot (Public Health Agency of Canada) for the WNV sample. The authors would like to thank Dr. Jill Kelly and Martin J. Richer, M.Sc., for proofreading and useful discussion of the manuscript. We would also like to thank Reg Sidhu for technical assistance (Leica Microsystems).

References

Amberg, S.M., Nestorowicz, A., McCourt, D.W., and Rice, C.M. (1994). NS2B-3 proteinase-mediated processing in the yellow fever virus structural region: *in vitro* and *in vivo* studies. J. Virol. *68*, 3794–3802.

Bazan, J.F. and Fletterick, R.J. (1989). Detection of a trypsin-like serine protease domain in flaviviruses and pestiviruses. Virology *171*, 637–639.

Bera, A.K., Kuhn, R.J., and Smith, J.L. (2007). Functional characterization of cis and trans activity of the Flavivirus NS2B-NS3 protease. J. Biol. Chem. *282*, 12883–12892.

Brinkworth, R.I., Fairlie, D.P., Leung, D., and Young, P.R. (1999). Homology model of the dengue 2 virus NS3 protease: putative interactions with both substrate and NS2B cofactor. J. Gen. Virol. *80*, 1167–1177.

Brinton, M.A. (2002). The molecular biology of West Nile Virus: a new invader of the western hemisphere. Annu. Rev. Microbiol. *56*, 371–402.

Cahour, A., Falgout, B., and Lai, C.J. (1992). Cleavage of the dengue virus polyprotein at the NS3/NS4A and NS4B/NS5 junctions is mediated by viral protease NS2B-NS3, whereas NS4A/NS4B may be processed by a cellular protease. J. Virol. *66*, 1535–1542.

Castle, E. and Wengler, G. (1987). Nucleotide sequence of the 5′-terminal untranslated part of the genome of the flavivirus West Nile virus. Arch. Virol. *92*, 309–313.

Castle, E., Nowak, T., Leidner, U., and Wengler, G. (1985). Sequence analysis of the viral core protein and the membrane-associated proteins V1 and NV2 of the flavivirus West Nile virus and of the genome sequence for these proteins. Virology *145*, 227–236.

Castle, E., Leidner, U., Nowak, T., and Wengler, G. (1986). Primary structure of the West Nile flavivirus genome region coding for all nonstructural proteins. Virology *149*, 10–26.

Centers for Disease Control and Prevention (1999). Outbreak of West Nile-like viral encephalitis – New York, 1999. Morb. Mortal. Wkly. Rep. *48*, 845–849.

Chambers, T.J., Hahn, C.S., Galler, R., and Rice, C.M. (1990a). Flavivirus genome organization, expression, and replication. Annu. Rev. Microbiol. *44*, 649–688.

Chambers, T.J., Weir, R.C., Grakoui, A., McCourt, D.W., Bazan, J.F., Fletterick, R.J., and Rice, C.M. (1990b). Evidence that the N-terminal domain of nonstructural protein NS3 from yellow fever virus is a serine protease responsible for site-specific cleavages in the viral polyprotein. Proc. Natl. Acad. Sci. USA *87*, 8898–8902.

Chambers, T.J., Grakoui, A., and Rice, C.M. (1991). Processing of the yellow fever virus nonstructural polyprotein: a catalytically active NS3 proteinase domain and NS2B are required for cleavages at dibasic sites. J. Virol. *65*, 6042–6050.

Chambers, T.J., Nestorowicz, A., Amberg, S.M., and Rice, C.M. (1993). Mutagenesis of the yellow fever virus NS2B protein: effects on proteolytic processing, NS2B-NS3 complex formation, and viral replication. J. Virol. *67*, 6797–6807.

Chambers, T.J., Nestorowicz, A., and Rice, C.M. (1995). Mutagenesis of the yellow fever virus NS2B/3 cleavage site: determinants of cleavage site specificity and effects on polyprotein processing and viral replication. J. Virol. *69*, 1600–1605.

Chappell, K.J., Nall, T.A., Stoermer, M.J., Fang, N.X., Tyndall, J.D., Fairlie, D.P., and Young, P.R. (2005). Site-directed mutagenesis and kinetic studies of the West Nile Virus NS3 protease identify key enzyme-substrate interactions. J. Biol. Chem. *280*, 2896–2903.

Chappell, K.J., Stoermer, M.J., Fairlie, D.P., and Young, P.R. (2006). Insights to substrate binding and processing by West Nile Virus NS3 protease through combined modeling, protease mutagenesis, and kinetic studies. J. Biol. Chem. *281*, 38448–38458.

Chappell, K.J., Stoermer, M.J., Fairlie, D.P., and Young, P.R. (2007). Generation and characterization of proteolytically active and highly stable truncated and full-length recombinant West Nile virus NS3. Protein Expr. Purif. *53*, 87–96.

Chappell, K.J., Stoermer, M.J., Fairlie, D.P., and Young, P.R. (2008a). Mutagenesis of the West Nile virus NS2B cofactor domain reveals two regions essential for protease activity. J. Gen. Virol. *89*, 1010–1014.

Chappell, K.J., Stoermer, M.J., Fairlie, D.P., and Young, P.R. (2008b). West Nile Virus NS2B/NS3 protease as an antiviral target. Curr. Med. Chem. *15*, 2771–2784.

Chernov, A.V., Shiryaev, S.A., Aleshin, A.E., Ratnikov, B.I., Smith, J.W., Liddington, R.C., and Strongin, A.Y. (2008). The two-component NS2B-NS3 proteinase represses DNA unwinding activity of the West Nile virus NS3 helicase. J. Biol. Chem. *283*, 17270–17278.

Clum, S., Ebner, K.E., and Padmanabhan, R. (1997). Cotranslational membrane insertion of the serine proteinase precursor NS2B-NS3(Pro) of dengue virus type 2 is required for efficient in vitro processing and is mediated through the hydrophobic regions of NS2B. J. Biol. Chem. *272*, 30715–30723.

Drebot, M.A., Lindsay, R., Barker, I.K., Buck, P.A., Fearon, M., Hunter, F., Sockett, P., and Artsob, H. (2003). West Nile virus

Author's Copy

Author's Copy

Author's Copy

Author's Copy

surveillance and diagnostics: a Canadian perspective. Can. J. Infect. Dis. *14*, 105–114.

Ezgimen, M.D., Mueller, N.H., Teramoto, T., and Padmanabhan, R. (2009). Effects of detergents on the West Nile virus protease activity. Bioorg. Med. Chem. *17*, 3278–3282.

Falgout, B. and Markoff, L. (1995). Evidence that flavivirus NS1-NS2A cleavage is mediated by a membrane-bound host protease in the endoplasmic reticulum. J. Virol. *69*, 7232–7243.

Gorbalenya, A.E., Donchenko, A.P., Koonin, E.V., and Blinov, V.M. (1989a). N-terminal domains of putative helicases of flavi- and pestiviruses may be serine proteases. Nucleic Acids Res. *17*, 3889–3897.

Gorbalenya, A.E., Koonin, E.V., Donchenko, A.P., and Blinov, V.M. (1989b). Two related superfamilies of putative helicases involved in replication, recombination, repair and expression of DNA and RNA genomes. Nucleic Acids Res. *17*, 4713–4730.

Grakoui, A., McCourt, D.W., Wychowski, C., Feinstone, S.M., and Rice, C.M. (1993). Characterization of the hepatitis C virus-encoded serine proteinase: determination of proteinase-dependent polyprotein cleavage sites. J. Virol. *67*, 2832–2843.

Hamill, P. and Jean, F. (2005). Enzymatic characterization of membrane-associated hepatitis C virus NS3-4A heterocomplex serine protease activity expressed in human cells. Biochemistry *44*, 6586–6596.

Hinson, E.R. and Cresswell, P. (2009). The antiviral protein, viperin, localizes to lipid droplets via its N-terminal amphipathic a-helix. Proc. Natl. Acad. Sci. USA *106*, 20452–20457.

Lin, C., Chambers, T.J., and Rice, C.M. (1993). Mutagenesis of conserved residues at the yellow fever virus 3/4A and 4B/5 dibasic cleavage sites: effects on cleavage efficiency and polyprotein processing. Virology *192*, 596–604.

Lindenbach, B.D., Thiel, H., and Rice, C.M. (2007). Flaviviridae: the viruses and their replication. In: Fields Virology, 5th edn, Vol. 1, D.M. Knipe and P.M. Howley, eds. (Philadelphia, PA, USA: Lippincott Williams and Wilkins), pp. 1101–1152.

Martin, M.M. and Jean, F. (2006). Single-cell resolution imaging of membrane-anchored hepatitis C virus NS3/4A protease activity. Biol. Chem. *387*, 1075–1080.

Nall, T.A., Chappell, K.J., Stoermer, M.J., Fang, N.X., Tyndall, J.D., Young, P.R., and Fairlie, D.P. (2004). Enzymatic characterization and homology model of a catalytically active recombinant West Nile virus NS3 protease. J. Biol. Chem. *279*, 48535–48542.

Radichev, I., Shiryaev, S.A., Aleshin, A.E., Ratnikov, B.I., Smith, J.W., Liddington, R.C., and Strongin, A.Y. (2008). Structure-based mutagenesis identifies important novel determinants of the NS2B cofactor of the West Nile virus two-component NS2B-NS3 proteinase. J. Gen. Virol. *89*, 636–641.

Rice, C.M., Lenches, E.M., Eddy, S.R., Shin, S.J., Sheets, R.L., and Strauss, J.H. (1985). Nucleotide sequence of yellow fever virus: implications for flavivirus gene expression and evolution. Science *229*, 726–733.

Richer, M.J., Juliano, L., Hashimoto, C., and Jean, F. (2004). Serpin mechanism of hepatitis C virus nonstructural 3 (NS3) protease inhibition: induced fit as a mechanism for narrow specificity. J. Biol. Chem. *279*, 10222–10227.

Schechter, I. and Berger, A. (1967). On the size of the active site in proteases. I. Papain. Biochem. Biophys. Res. Commun. *27*, 157–162.

Shiryaev, S.A., Ratnikov, B.I., Chekanov, A.V., Sikora, S., Rozanov, D.V., Godzik, A., Wang, J., Smith, J.W., Huang, Z., Lindberg, I., et al. (2006). Cleavage targets and the D-arginine-based inhibitors of the West Nile virus NS3 processing proteinase. Biochem. J. *393*, 503–511.

Shiryaev, S.A., Aleshin, A.E., Ratnikov, B.I., Smith, J.W., Liddington, R.C., and Strongin, A.Y. (2007a). Expression and purification of a two-component flaviviral proteinase resistant to autocleavage at the NS2B-NS3 junction region. Protein Expr. Purif. *52*, 334–339.

Shiryaev, S.A., Kozlov, I.A., Ratnikov, B.I., Smith, J.W., Lebl, M., and Strongin, A.Y. (2007b). Cleavage preference distinguishes the two-component NS2B-NS3 serine proteinases of Dengue and West Nile viruses. Biochem. J. *401*, 743–752.

Shiryaev, S.A., Ratnikov, B.I., Aleshin, A.E., Kozlov, I.A., Nelson, N.A., Lebl, M., Smith, J.W., Liddington, R.C., and Strongin, A.Y. (2007c). Switching the substrate specificity of the two-component NS2B-NS3 flavivirus proteinase by structure-based mutagenesis. J. Virol. *81*, 4501–4509.

Uchil, P.D. and Satchidanandam, V. (2003). Architecture of the flaviviral replication complex. Protease, nuclease, and detergents reveal encasement within double-layered membrane compartments. J. Biol. Chem. *278*, 24388–24398.

Wengler, G. (1991). The carboxy-terminal part of the NS 3 protein of the West Nile flavivirus can be isolated as a soluble protein after proteolytic cleavage and represents an RNA-stimulated NTPase. Virology *184*, 707–715.

Wengler, G., Nowak, T., and Castle, E. (1990). Description of a procedure which allows isolation of viral nonstructural proteins from BHK vertebrate cells infected with the West Nile flavivirus in a state which allows their direct chemical characterization. Virology *177*, 795–801.

Wengler, G., Czaya, G., Farber, P.M., and Hegemann, J.H. (1991). *In vitro* synthesis of West Nile virus proteins indicates that the amino-terminal segment of the NS3 protein contains the active centre of the protease which cleaves the viral polyprotein after multiple basic amino acids. J. Gen. Virol. *72*, 851–858.

Yamshchikov, V.F. and Compans, R.W. (1993). Regulation of the late events in flavivirus protein processing and maturation. Virology *192*, 38–51.

Yamshchikov, V.F. and Compans, R.W. (1994). Processing of the intracellular form of the west Nile virus capsid protein by the viral NS2B-NS3 protease: an *in vitro* study. J. Virol. *68*, 5765–5771.

Yamshchikov, V.F., Trent, D.W., and Compans, R.W. (1997). Upregulation of signalase processing and induction of prM-E secretion by the flavivirus NS2B-NS3 protease: roles of protease components. J. Virol. *71*, 4364–4371.

Yu, I.M., Zhang, W., Holdaway, H.A., Li, L., Kostyuchenko, V.A., Chipman, P.R., Kuhn, R.J., Rossmann, M.G., and Chen, J. (2008). Structure of the immature dengue virus at low pH primes proteolytic maturation. Science *319*, 1834–1837.

Yusof, R., Clum, S., Wetzel, M., Murthy, H.M., and Padmanabhan, R. (2000). Purified NS2B/NS3 serine protease of dengue virus type 2 exhibits cofactor NS2B dependence for cleavage of substrates with dibasic amino acids *in vitro*. J. Biol. Chem. *275*, 9963–9969.

Received October 25, 2009; accepted January 25, 2010

Author's Copy

Author's Copy

Author's Copy